JOURNAL OF AIRCRAFT
Vol. 31, No. 3, May–June 1994

Computation of Supersonic Jet Mixing Noise for an Axisymmetric Convergent-Divergent Nozzle

Abbas Khavaran*
Sverdrup Technology, Inc., Lewis Research Group, Cleveland, Ohio 44135
and
Eugene A. Krejsa† and Chan M. Kim‡
NASA Lewis Research Center, Cleveland, Ohio 44135

The turbulent mixing noise of a supersonic jet is calculated for an axisymmetric convergent-divergent nozzle at the design pressure ratio. Aerodynamic computations are performed using the PARC code with a k-ε turbulence model. Lighthill's acoustic analogy is adopted. The acoustics solution is based upon the methodology followed in the MGB code. The source correlation function is expressed as a linear combination of second-order tensors (Ribner's assumption). Assuming separable second-order correlations and incorporating Batchelor's isotropic turbulence model, the source term was calculated from the kinetic energy of turbulence. A Gaussian distribution for the time-delay of correlation was introduced. The CFD solution was used to obtain the source strength as well as the characteristic time-delay of correlation. The effect of sound/flow interaction was incorporated using the high frequency asymptotic solution to Lilley's equation for axisymmetric geometries. Acoustic results include sound pressure level directivity and spectra at different polar angles. The aerodynamic and acoustic results demonstrate favorable agreement with experimental data.

Nomenclature

C, C_∞	=	local and ambient speeds of sound
$\bar{C}$	=	convection factor
D, D_{eq}	=	exit and throat diameters
f	=	observed frequency
I_{ijkl}	=	source correlation tensor
K	=	wave number
k	=	turbulent kinetic energy, $\overline{v_i v_i}/2$
L	=	longitudinal macroscale of turbulence
L_e	=	eddy length scale
M, M_j	=	local and exit Mach numbers
M_c, M_∞	=	convection and flight Mach numbers
R	=	source to observer distance
R_i	=	observer coordinate
r	=	radial distance
T	=	intensity of turbulence, $\overline{v_i v_i}/3$
T_{ij}	=	unsteady momentum flux
U	=	mean velocity in direction of flow
U_j	=	exit jet velocity
V_i	=	local velocity component
v_i	=	fluctuating velocity component in X_i direction
$\overline{v_i v_j'}$	=	two-points time-delayed second-order correlation, $\int_{-\infty}^{+\infty} v_i(y, t)v_j(y + \xi, t + \tau)\, dt$
y	=	source coordinate
α_c, β_c	=	convection constants
α_f	=	proportionality factor, $1/\tau_0 = \alpha_f \varepsilon/k$
δ_{ij}	=	Kronecker's delta
ε	=	dissipation rate of kinetic energy, $\nu(\partial v_i/\partial X_j)(\partial v_i/\partial X_j)$
θ	=	polar angle with respect to downstream axis
Λ	=	source factor
ν	=	molecular viscosity
ξ	=	vector separation of correlation
ρ, ρ_∞	=	local and ambient densities
τ	=	time delay of correlation
τ_0	=	characteristic time delay of correlation
ϕ	=	azimuthal angle
ω, Ω	=	observer and source radian frequencies

Presented as Paper 92-0500 at the AIAA 30th Aerospace Sciences Meeting and Exhibit, Reno, NV, Jan. 6–9, 1992; received June 25, 1992; revision received May 3, 1993; accepted for publication May 11, 1993.

*Senior Research Engineer. Member AIAA.
†Deputy Branch Chief, Propeller and Acoustic Technology Branch. Member AIAA.
‡Aerospace Engineer. Member AIAA.

I. Introduction

RECENT advances in the area of computational fluid dynamics have provided researchers with new tools for approaching aeroacoustic problems. The direct computation of the sound field based on the solution to full, unsteady, compressible Navier-Stokes equations is the ultimate goal in an area which has been labeled as computational aeroacoustics. However, the limitations of the available computational resources require a more practical approach. Such an approach is taken here to study high-speed jet noise because of current interest in high speed civil transport (HSCT).

Over a decade ago, a unified aerodynamic/acoustic prediction code (MGB code) was developed by Mani et al.[1] The aerodynamic predictions within this code are carried out by applying an extension of Reichardt's model.[2] The three components of turbulent shearing stress are computed based upon contour integrals around the nozzle exit geometry and utilized in deriving an expression for the source strength. Though the closed form nature of Reichardt's solution has led to a versatile and relatively fast numerical scheme, the assumptions inherent in the derivations render inaccurate aerodynamic prediction for complex geometries.

Reichardt's solution essentially assumes exhaust nozzle elements discharge axially. It neglects radial mean flow and swirl, and does not take into account the effect of shock structure on mixing and turbulence. These assumptions, among others, could vitiate the acoustic predictions substantially, especially for new lobed hypermix nozzles that are the present focus in HSCT research. To circumvent some of the pitfalls associated with Reichardt's model, a two-stage algorithm was employed. The aerodynamic calculations are carried out independently and the resulting time-averaged properties are used for noise prediction. The following computational advantages are associated with a two-stage algorithm:

1) The aerodynamic calculations can start from within the nozzle, giving a more realistic model of the exit conditions.

2) Grid selection can be done independently for aerodynamic and acoustic purposes. The plume is treated as an integration of axial slices in the acoustic computations.

3) Proper prediction of shock-cell structure as well as shock intensity is essential in prediction of the shock-associated noise. This subject is not discussed here due to the absence of the shock-associated noise.

The geometry considered in this article is a round convergent-divergent nozzle. This particular nozzle has previously been tested aerodynamically and acoustically for NASA Lewis by General Electric.[3] Test data has been especially helpful in assessing the CFD results before proceeding with noise computations. The flow path is designed to obtain an isentropic, uniform, and parallel flow at the nozzle exit for the design Mach number of 1.4, thereby eliminating to a large degree, any shock-induced noise. An axisymmetric version of the PARC code[4] with Chien's k-ε turbulence model[5] has been used. The complete Reynolds-averaged Navier-Stokes equations are solved in conservative law form. The Beam and Warming approximate factorization algorithm is used for forming the implicit central-difference algorithm (see Ref. 4). A Baldwin and Lomax style algebraic turbulence model is utilized to compute the boundary values and initial conditions for k and ε. The viscous coefficients are determined based on Sutherland's viscosity law, Stokes hypothesis, and constant Prandtl number assumption. The predicted flowfield is compared with data as well as solutions from Reichardt's model.

II. Method of Solution

The solution technique is essentially based upon the methodology followed by Mani et al.[1] in the MGB code. Reichardt's aerodynamic model is replaced with CFD and the technique is briefly outlined here with emphasis on the new changes and comparisons with the original model.

The solution technique is described in two sections: 1) source spectrum model and 2) sound/flow interaction. The first section describes the application of PARC with a k-ε turbulence model to the computation of source strength and its spectrum. Empirical constants used in the computation of characteristic Strouhal number and supersonic convection factor are described. In the second section, the effect of the surrounding medium (temperature and velocity gradients) on the noise radiated from convecting quadrupole sources is discussed.

A. Source Spectrum Model

The mean-square pressure autocorrelation in the far field—in the absence of convection and refraction—is written using Lighthill's acoustic analogy approach[6,7]:

$$\overline{p^2}(R, \theta, \phi, \tau) = \frac{R_iR_jR_kR_l}{16\pi^2C_\infty^4R^6}\int_y\int_\xi \frac{\partial^4}{\partial\tau^4}\overline{T_{ij}T'_{kl}}\,\mathrm{d}\xi\,\mathrm{d}y \quad (1)$$

The source strength is assumed to be dominated by unsteady momentum flux, i.e., $T_{ij} \sim \rho V_iV_j$. R is the magnitude of the source/observer vector and its three components are represented as R_i for $i = 1, 2, 3$. Vector $\boldsymbol{\xi}$ in the above integration is the separation vector of the correlation between ρV_iV_j computed at y and $\rho' V'_kV'_l$ at $y + \boldsymbol{\xi}$ and τ is the time-delay of correlation. The corresponding spectrum can be expressed in terms of the Fourier transform of the autocorrelation function

$$\overline{p^2_\omega} = \frac{1}{2\pi}\int_{-\infty}^{+\infty}\overline{p^2}e^{i\omega\tau}\,\mathrm{d}\tau \quad (2)$$

As such, for a quasi-incompressible turbulence, the source strength is characterized by a two-point time-delayed fourth-order velocity correlation tensor. For a nearly parallel mean flow, the constituent velocities may be written as the sum of the local mean velocity and the turbulent velocity, $V_i = U\delta_{i1} + v_i$. Substituting V_i into Eq. (1), the contribution to the integral due to the self noise terms is shown to be independent of the mean flow. This contribution, as shown by Ribner,[8] is primarily due to terms like $\overline{v_iv_jv'_kv'_l}$. As explained by Mani,[9] the distinction between shear noise and self noise becomes less important when the interpretation of the source terms is based upon Lilley's[10] formulation rather than Lighthill's equation. Assuming a normal joint probability for turbulent velocity components and using the isotropic turbulence model of Batchelor,[11] the fourth-order correlation can be written as a linear combination of second-order correlations:

$$\overline{v_iv_jv'_kv'_l} = (\overline{v_iv'_k})(\overline{v_jv'_l}) + (\overline{v_iv'_l})(\overline{v_jv'_k}) + (\overline{v_iv'_j})(\overline{v_kv'_l}) \quad (3)$$

The latter expression is true if the third-order correlation functions would vanish. It is known that the triple correlations do not vanish in a homogeneous turbulence, however, based on experimental observations,[12] Eq. (3) is still a good approximation. Furthermore, by assuming that the two-point velocity correlations $\overline{v_iv'_j}$ are separable in space/time factors, as postulated by Ribner

$$\overline{v_iv'_j} = R_{ij}(\boldsymbol{\xi})g(\tau) \quad (4)$$

the integration on separation vector of correlation can be carried out in closed form. The space factor appropriate to homogeneous isotropic turbulence[11] is given as

$$R_{ij}(\boldsymbol{\xi}) = T[(f + \tfrac{1}{2}\xi f')\delta_{ij} - \tfrac{1}{2}f'\xi_i\xi_j/\xi] \quad (5)$$

where $T = \frac{1}{3}\overline{v_iv_i}$ is the intensity of turbulence, and $f' = \partial f/\partial\xi$. The three components of the separation vector of correlation are represented as ξ_i for $i = 1, 2, 3$. Function $f(\xi)$ can be expressed as $f(\xi) = \exp(-\pi\xi^2/L^2)$. This expression makes $f(\xi)$ decrease to zero for large ξ with sufficient rapidity to make $\int_0^\infty \xi^m f(\xi)\,\mathrm{d}\xi$ converge for $m \geq 0$. Length L is the longitudinal macroscale of turbulence, representing the linear extent of the region within which velocities are appreciably correlated. The time factor of correlation is expressed as $g(\tau) = \exp(-\tau^2/\tau_0^2)$, where τ_0 denotes the characteristic time-delay in a moving reference frame. For axisymmetric jets, Davies et al.[13] have shown that τ_0 is proportional to the inverse of mean shear, i.e., $1/\tau_0 \sim (\partial U/\partial r)$. In addition, turbulence intensity can be expressed in terms of L and τ_0 according to $\tau_0 \sim L/\sqrt{T}$. Since L_ε is related to kinetic energy of turbulence $k = \overline{v_iv_i}/2$, and its dissipation rate ε as $L_\varepsilon = k^{3/2}/\varepsilon$, assuming that L_ε and L are proportional, it can be concluded that $1/\tau_0 \sim \varepsilon/k$. Comparison of τ_0, as computed from k and ε, with the corresponding results obtained from the velocity gradient and Reichardt's aerodynamic solution, are presented under the numerical discussions.

Ribner[8] evaluates the contribution to self noise for various source strength components. The corresponding spectrum is evaluated by using a Fourier transform on the time-delay of the correlation. The first component of source/spectrum correlation tensor is

$$I_{1111}(\Omega) = (3/8\sqrt{\pi})\rho^2k^{7/2}(\Omega\tau_0)^4e^{[-(\Omega\tau_0)^2/8]} \quad (6)$$

The remaining components are expressed similarly (see the Appendix). To account for the refraction of sound due to the mean flow, each correlation tensor will be multiplied by the corresponding directivity factor. The Doppler effect relating the source frequency Ω and f is expressed as $\Omega = 2\pi f\tilde{C}$. The singular behavior of the eddy convection factor $\tilde{C} = (1 - M_c\cos\theta)$ at supersonic convection speeds ($M_c > 1$) has been discussed by Ffowcs Williams.[14] The autocorrelation function in this region, which corresponds to emission of eddy Mach wave, becomes zero, and therefore the integrand remains finite. In our analysis, a modified convection factor described by

$$\bar{C} = \sqrt{(1 - M_c \cos\theta)^2 + (\alpha_c k^{0.5}/C_\infty)^2} \tag{7}$$

has been selected for numerical computation. The empirical convection constant α_c was determined from comparison of prediction with data. A value of $\alpha_c = 0.5$ is generally a good approximation for most observation angles. The convection Mach number was expressed as a function of the weighted average of the nozzle exit Mach number and local Mach M:

$$M_c = 0.5M + \beta_c M_j \tag{8}$$

Values in the range of 0.25–0.3 for the convection constant β_c appear to yield best results.

B. Sound/Flow Interaction

Lighthill's acoustic analogy approach, based on classical wave equation does not incorporate the effect of surrounding mean flow on the sound radiated by convected multipole sources. It is clear that these pressure fluctuations propagate through a region of nonuniform velocity and temperature before reaching the observer point. Thus, the location of the source within the jet plume has a strong effect on the amount of the radiated sound. The mean flow results in not only the refraction of the radiated sound, but also an additional convection amplification due to fluid motion. A number of investigators have studied the radiation field of multipole sources immersed in parallel sheared flows. Mani[9,15,16] studied the mean flow interaction of round jets for slug flow profiles assuming quadrupole sources convecting along the centerline of the jet. Gliebe and Balsa[17] and Goldstein[18] extended the above analysis to arbitrary velocity profiles in high-frequency and low-frequency limits, respectively. The generalization to arbitrarily located sources in continuously varying monotonic profiles were derived by Balsa[19] and Goldstein.[20,21] For supersonic jets, the high-frequency solution provides an adequate approximation as suggested by Tester and Morfey[22] and Pao.[23]

Lilley's equation is considered as the starting point by most recent investigators studying the sound/flow interactions. For a parallel flow, the Green's function solution to a convected monopole of frequency Ω is obtained by applying a sequence of Fourier transformations. The solution corresponding to multipole singularities are obtained by differentiating the monopole solution with respect to appropriate source coordinate; once in the case of a dipole source and twice for quadrupole sources. Mani et al.[1] provide a comprehensive analysis of the shielding effect of an axisymmetric mean flow, i.e., when the jet velocity and temperature profiles are arbitrary functions of the radial variable. To study the effect of asymmetry in the mean flow, Goldstein[24] solves Lilley's equation for high-frequency multipole sources in a jet flow whose Mach number and temperature are functions of crossflow coordinates. This leads to an ordinary differential equation that traces the cross-stream projection of an acoustic ray starting from any given source location. The differential equation is solved repeatedly as one selects initial departure angle for rays leaving the source. Subsequent ray tracing through the shear layer and study of the spreading or focusing of the acoustic emission as it approaches far field, results in a circumferential directivity factor for each source volume element.

For the present axisymmetric geometry, Mani and Balsa's formulation for the sound/flow interaction is adopted. This is accomplished by coupling the turbulent properties of the jet with its acoustic radiation (see the Appendix). Thus, the mean square pressure in the far field is expressed as

$$\overline{p^2}(R, \theta, \Omega) = \int_y \Lambda(a_{xx} + 4a_{xy} + 2a_{yy} + 2a_{yz})\, \mathrm{d}y \tag{9}$$

The contribution to the noise field due to each of the quadrupoles contained within a turbulent eddy volume element is described by the directivity factors $a_{xx}, \ldots, a_{yz}$. Λ is a factor related to the source intensity and frequency

$$\Lambda \sim \frac{(\rho_\infty/\rho)^2 I_{1111}(\Omega)}{(4\pi R C_\infty C)^2 (1 - M\cos\theta)^2 (1 - M_c \cos\theta)^2} \tag{10}$$

The directivity factors are functions of the shielding function g^2, which is expressed in terms of the polar observation angle θ, local sound velocity C, and Mach numbers $M(r) = U(r)/C_\infty$ and $M_c = U_c/C_\infty$:

$$g^2(r) = \frac{(1 - M\cos\theta)^2 (C_\infty/C)^2 - \cos^2\theta}{(1 - M_c\cos\theta)^2} \tag{11}$$

The flow variables, as obtained from CFD, are used in the computation of $g^2(r)$, and therefore, the directivity factors $a_{xx}, \ldots, a_{yz}$. The location r, where $g^2(r)$ changes in sign, is called transition point or turning point. When $g^2(r)$ is negative between the source and observer, the possibility of fluid shielding exists. The position of the source with respect to the turning points of $g^2(r)$ contributes to the amount of fluid shielding through factor $\exp[-2K \int_{r_0}^{r_{tr}} \sqrt{|g^2(r)|}\, \mathrm{d}r]$, as explained in the Appendix.

The wave number $K = \Omega/C_\infty$, in the above exponential factor, tends to increase the attenuation of the high frequencies. A maximum of four turning points has been considered in the present computations. A correction of Doppler factor has been utilized for source volume effects according to Ffowcs Williams.[14] The correction for flight speed has been included using the flight dynamic factor $(1 + M_\infty \cos\theta)^{-1}$, where M_∞ is the flight Mach number.

III. Numerical Results and Discussion

To obtain the flowfield solution, a 141 × 60 grid (Fig. 1), highly clustered around the jet lip-line was used. A run time of over 4 h on the Cray Y-MP was required to achieve the necessary convergence based on residual reduction method. The aerodynamic results obtained from the PARC-$k\varepsilon$ code were used for noise computation. Both aerodynamic and

Table 1 Design parameters for C-D nozzle

Throat diameter	5.1 in.
Exit diameter	5.395 in.
Distance from throat to exit	5.525 in.
Exit velocity	2409 fps
Ambient velocity	400 fps
Pressure ratio	3.121
Stagnation temperature	1716°R

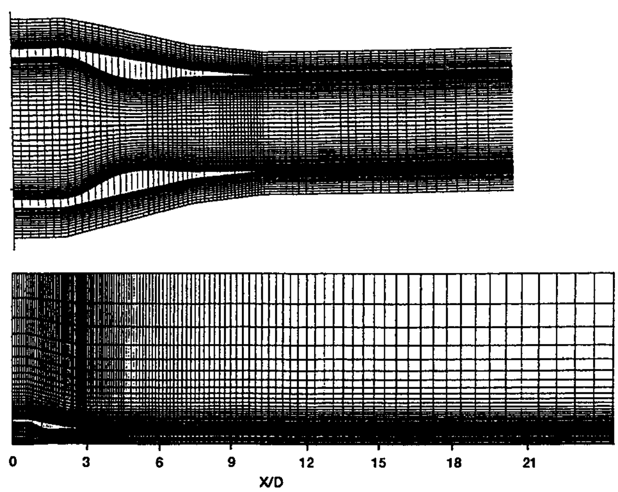

Fig. 1 Nozzle geometry and grid.

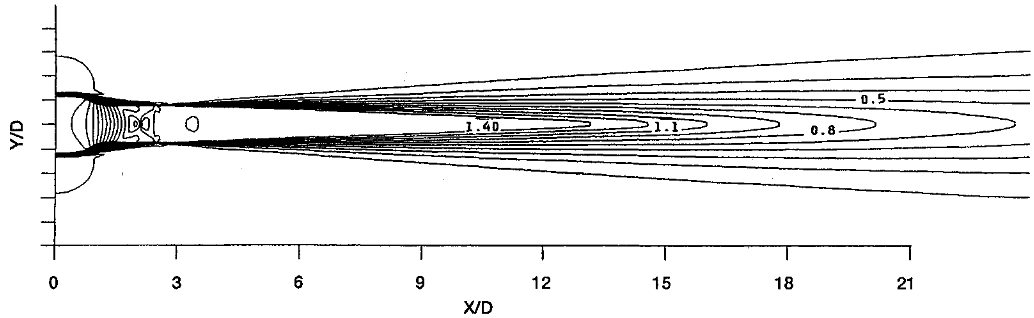

Fig. 2 Mach number contour plot (M_j = 1.4).

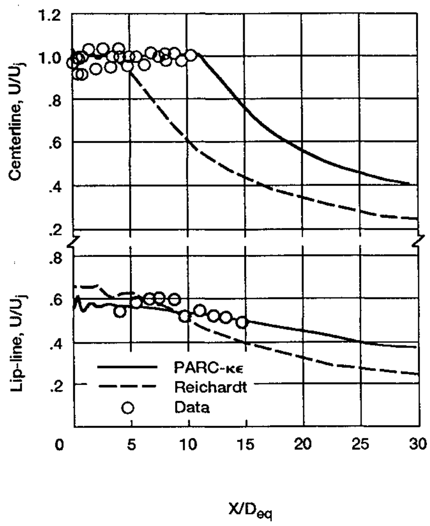

Fig. 3 Axial velocity component along nozzle lip-line and centerline.

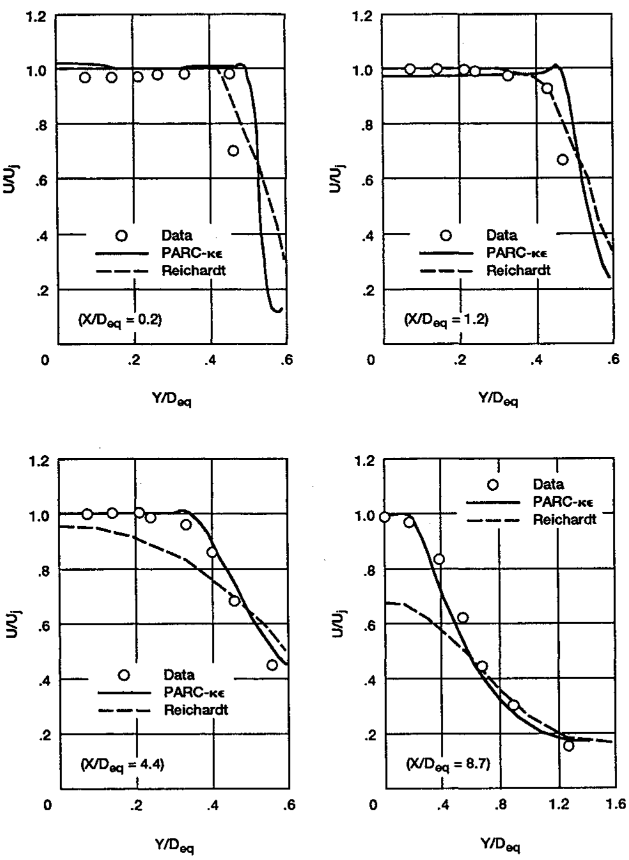

Fig. 4 Radial profile for axial velocity.

acoustic predictions were compared with available data. In addition, turbulent intensity and characteristic Strouhal number as predicted by the PARC code were compared with Reichardt's solution. All laser velocimeter, shadowgraph, and acoustic tests for this model were conducted in the General Electric anechoic free-jet facility.[3] The test point (corresponding to the design condition) is listed in Table 1. The Mach contour plot (Fig. 2) indicates the formation of a Mach disc inside the nozzle as well as a weak shock outside the exit plane.

Figure 3 shows the axial velocity component along the nozzle lip-line and centerline. The PARC predictions are in good agreement with data. The radial profile for axial velocity is given in Fig. 4 at four axial positions along the jet. Figure 5 exhibits the contour plot for the intensity of turbulence, indicating the extension of noise sources to nearly 18 diameters downstream. The contour levels are nondimensionalized with respect to reference sound speed a_r^2, which is computed at the stagnation temperature. Further details of the turbulence intensity distribution are demonstrated in Figs. 6 and 7. The axial distribution of the turbulence intensity near the lip-line (Fig. 6a) shows a level of 13% near the exit plane, with a growing decay rate after 12 nozzle diameters, generally in good agreement with data. Reichardt's model predicts a much faster decay after 5 diameters. The radial distribution (Fig. 6b) was plotted only at X/D = 8.21, where test data was available for comparison. Obviously, the PARC code does a better job in predicting the maximum turbulence level. Near the centerline, which is still within the potential core, the CFD computations clearly underpredict the data by 3–4%. This should not introduce any significant error in noise computation because of the low level of source intensity and high shielding effect. Further comparison of the predicted source term using the two aerodynamic prediction schemes is illustrated in Fig. 7. Reichardt's model obviously predicts a faster spreading. In addition, this prediction scheme does not accurately predict the axial decay of the turbulence intensity (see Fig. 6a).

The characteristic time-delay τ_0 was obtained using the two different definitions alluded to earlier. The corresponding characteristic Strouhal numbers defined as $(\varepsilon/k)(D/U_j)$ and $(\partial U/\partial r)(D/U_j)$ are plotted in Fig. 8. Figures 8a and 8b are both based on the PARC predictions. It is clear that outside the α_f needed for the computation of τ_0, these curves demonstrate remarkable resemblance, showing a peak value moving in toward the centerline with increasing X. Figure 8c, based on Reichardt's solution, shows the same general features, but fails to properly predict the radial location of the maximum. In our acoustic computations, τ_0 was calculated from $1/\tau_0 = \alpha_f \varepsilon/k$. The empirical factor α_f can shape the sound spectrum in terms of the location of the maximum. A value of α_f = 2 was selected in these calculations. For nonaxisymmetric geometries, additional modification in the definition of τ_0 is necessary as the circumferential gradient of the mean velocity also contributes to this factor.

The acoustic computations for a 40-ft radius are presented in Figs. 9 and 10. The overall sound pressure (OASPL) di-

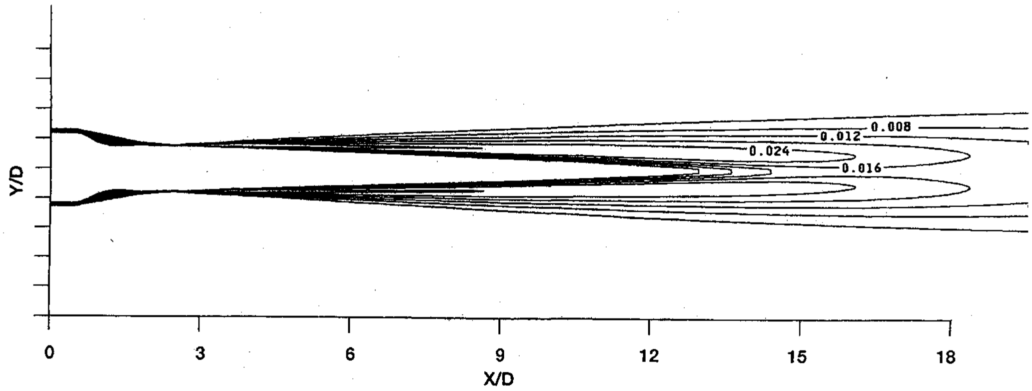

Fig. 5 Turbulent intensity contour plot (PARC-$k\varepsilon$).

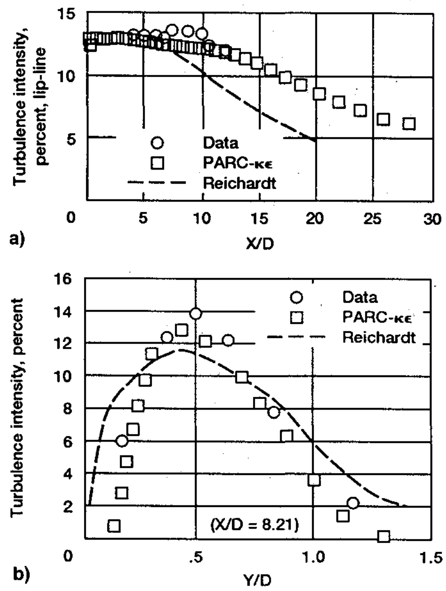

Fig. 6 Comparison between predicted turbulent intensity and experiment[3]: a) lip-line and b) $X/D = 8.21$.

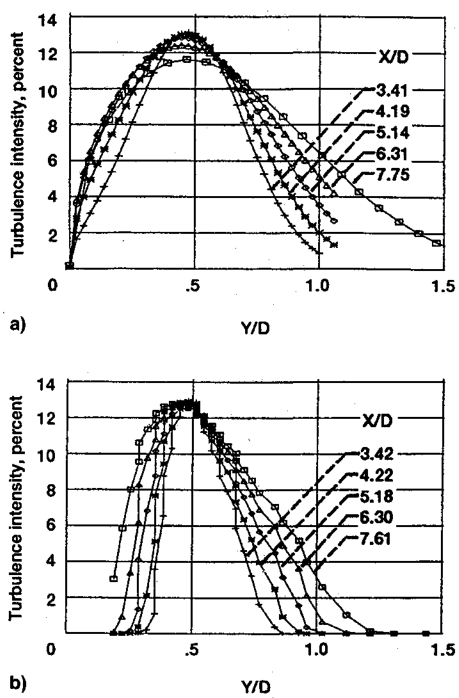

Fig. 7 Comparison of turbulent intensity profiles using two prediction methods: a) Reichardt's model and b) PARC-$k\varepsilon$.

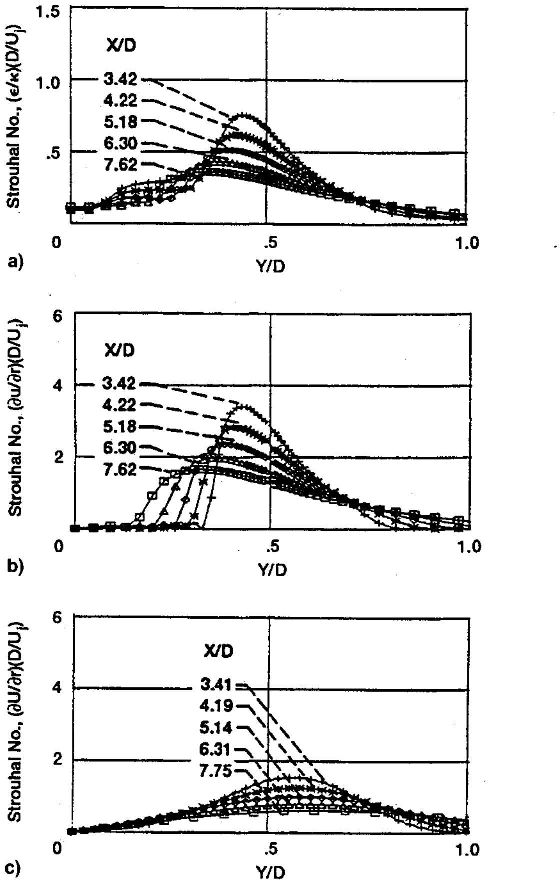

Fig. 8 Characteristic Strouhal no.: a) defined as $(\varepsilon/k)(D/U_j)$ obtained from PARC-$k\varepsilon$, b) defined as $(\partial U/\partial r)(D/U_j)$ obtained from PARC-$k\varepsilon$, and c) same as b), but obtained from Reichardt's model.

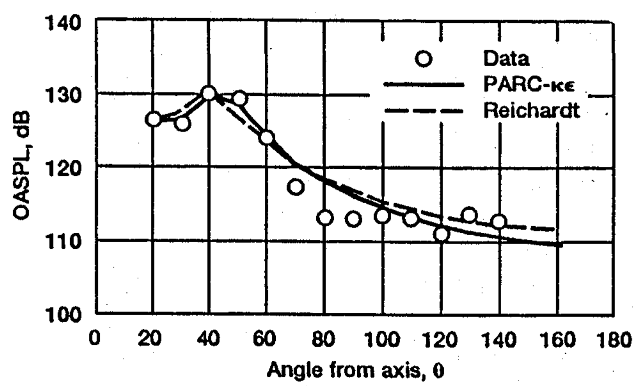

Fig. 9 Comparison of the overall sound pressure level directivity with data[3] on a 40-ft radius.

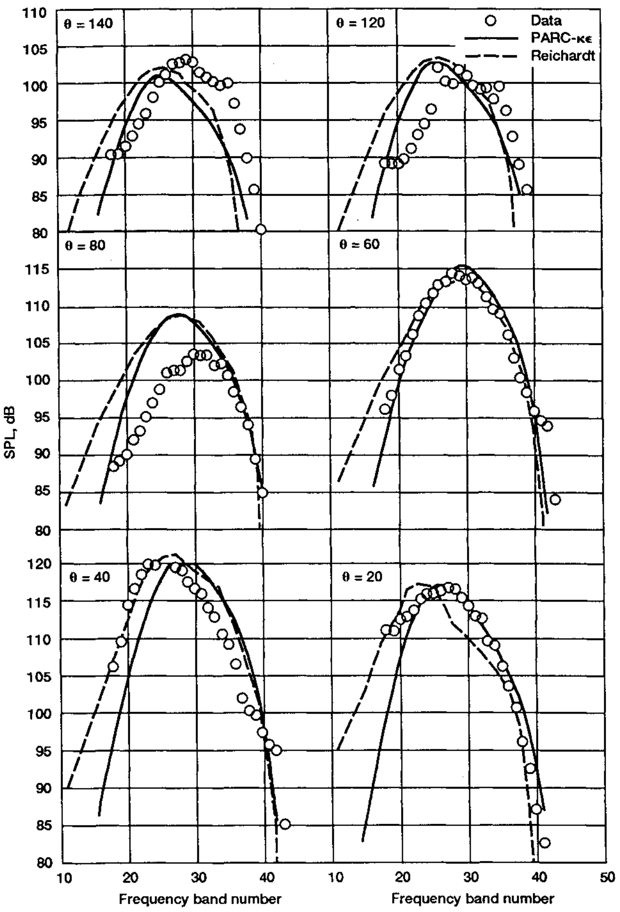

Fig. 10 Comparison of the spectral components of noise with data[3] based on a one-third octave center frequency (band number 11 corresponds to 50 Hz).

rectivity as obtained from the PARC shows reasonable agreement with data at most observation angles. The selected value of α_f results in good agreement in downstream directions, where the jet mixing noise is dominant. Obviously, for off-design conditions, the shock-associated noise dominates at angles close to upstream axis and several decibal's difference in our predictions would not significantly alter the directivity of the total noise. The overprediction of up to 5 dB at θ = 80 deg can be improved by selecting an angle-dependent convection constant α_c in Eq. (7). Reichardt's solution also generates results in close agreement with data as the empirical constants used in the corresponding unified aeroacoustic code are calibrated for a conical flowfield. The spectral components of noise, based on a one-third octave band are shown in Fig. 10. The overall agreement seems acceptable.

IV. Conclusions

The source strength of supersonic jet mixing noise has been predicted using the PARC code with a k-ε turbulence model. The noise predictions compare reasonably with experimental data. This application has removed four empirical constants used in the Reichardt's model, which are calibrated for a conical flowfield. The limitations on aerodynamic grid selection has been removed by adopting a two-stage aerodynamic and acoustic algorithm. Furthermore, the time-delay of correlation has been computed using two different models. The acoustic computations in the present model are based on two fundamental assumptions as suggested by Ribner[8] and Batchelor.[11] A proper prediction of the noise spectrum is sensitive to an accurate assessment of the characteristic Strouhal number of the correlation volume element.

For nonaxisymmetric geometries, a proper circumferential averaging of the flow variables can be used as a first step in the computation of the polar directivity of jet noise. Contributions from other components of the mean velocity gradient should also be included in the computation of τ_0. More elaborate analysis such as geometric ray theory will be needed to predict the circumferential directivity of jet noise. In addition, the empirical constants introduced in the determination of supersonic convection factor should be further investigated for other geometries.

Appendix

The contributions to self noise due to various components of source correlation tensor I_{ijkl} are

$$I_{1111} = I_{2222} = I_{3333} = 8I_{1122} = 8I_{1133} = 8I_{2233}$$

$$I_{1212} = I_{1313} = I_{2323} = \tfrac{7}{16} I_{1111} \qquad \text{(A1)}$$

The remaining elements are either redundant (e.g., $I_{1212} = I_{2121}$), or have no contribution. The sound/flow interaction for an arbitrary eddy volume element is obtained by multiplying each correlation component by the corresponding directivity factor

$$I_{1111}a_{xx} + I_{2222}a_{yy} + I_{3333}a_{zz} + (2I_{1122} + 4I_{1212})a_{xy} + (2I_{1133} + 4I_{1313})a_{xz} + (2I_{2233} + 4I_{2323})a_{yz} \qquad \text{(A2)}$$

The weighting factors 2 and 4 result from permutation of $ijkl$. For an axisymmetric flow with x corresponding to the streamwise direction ($a_{yy} = a_{zz}, a_{xz} = a_{xy}$), Eq. (A2) can be simplified as $I_{1111}(a_{xx} + 2a_{yy} + 4a_{xy} + 2a_{yz})$. The directivity factors for various convecting quadrupole source components are (see Ref. 25)

$$a_{xx} = \frac{\cos^4\theta\beta_{xx}}{(1 - M_c\cos\theta)^4}, \qquad a_{xy} = \frac{g_0^2\cos^2\theta\beta_{xy}}{2(1 - M_c\cos\theta)^2}$$

$$a_{yy} = \tfrac{3}{8}g_0^4\beta_{yy}, \qquad a_{yz} = \tfrac{1}{8}g_0^4\beta_{yz} \qquad \text{(A3)}$$

where g_0^2 is the value of the shielding function $g^2(r)$ at the source location r_0. When g^2 is negative, a shielding zone exists. The amount of shielding depends upon the location of source with respect to the turning point of g^2, as well as the number of turning points. This dependence is incorporated through shielding coefficients $\beta_{xx}, \beta_{yy}, \ldots$. For example, when there is only one turning point r_{t1}, the shielding coefficients become constant multipliers of $\exp[-2K\int_{r_0}^{r_{t1}}\sqrt{|g^2(r)|}\,dr]$. For a complete listing of β_{ij} for various source correlation elements and their dependence on the number of turning points, see Refs. 1 and 25.

References

[1]Mani, R., et al., "High Velocity Jet Noise Source Location and Reduction," Task 2, FAA-RD-76-79-II, May 1978.

[2]Reichardt, H., "On a New Theory of Free Turbulence," *Royal Aeronautical Society Journal*, Vol. 47, June 1943, pp. 167–176.

[3]Yamamoto, K. J., et al., "Experimental Investigation of Shock-Cell Noise Reduction for Single Stream Nozzles in Simulated Flight—Comprehensive Data Report," NASA CR-168234, Dec. 1984.

[4]Cooper, G. K., and Sirbaugh, J. R., "PARC Code: Theory and Usage," Arnold Engineering Development Center, AEDC-TR-89-15, Dec. 1989.

[5]Chien, K. Y., "Prediction of Channel and Boundary Layer Flows with a Low Reynolds-Number Turbulence Model," *AIAA Journal*, Vol. 20, No. 1, 1982, pp. 33–38.

[6]Lighthill, M. J., "On Sound Generated Aerodynamically. I General Theory," *Proceedings of the Royal Society of London*, Vol. A211, March 1952, pp. 564–587.

[7]Lighthill, M. J., "On Sound Generated Aerodynamically. II Turbulence as a Source of Sound," *Proceedings of the Royal Society of London*, Vol. A222, Feb. 1954, pp. 1–32.

[8]Ribner, H. S., "Quadrupole Corrections Governing the Pattern of Jet Noise," *Journal of Fluid Mechanics*, Vol. 38, Aug. 1969, pp.

1–24.

[9]Mani, R., "The Influence of Jet Flow on Jet Noise, Part I, The Noise of Unheated Jets," *Journal of Fluid Mechanics*, Vol. 76, Feb. 1976, pp. 753–778.

[10]Lilley, G. M., Morris, P. J., and Tester, B. J., "On the Theory of Jet Noise and Its Application," AIAA Paper 73-987, Oct. 1973.

[11]Batchelor, G. K., *The Theory of Homogeneous Turbulence*, Cambridge Univ. Press, Cambridge, MA, 1953.

[12]Lin, C. C., *Statistical Theories of Turbulence*, Princeton Univ. Press, Princeton, NJ, 1961.

[13]Davies, P. O. A. L., Fisher, M. J., and Barratt, M. J., "The Characteristics of the Turbulence in the Mixing Region of a Round Jet," *Journal of Fluid Mechanics*, Vol. 15, March 1963, pp. 337–367.

[14]Ffowcs Williams, J. E., "The Noise from Turbulence Convected at High Speed," *Philosophical Transactions of the Royal Society of London*, Vol. A255, April 1963, pp. 469–503.

[15]Mani, R., "Moving Source Problem Relevant to Jet Noise," *Journal of Sound and Vibration*, Vol. 25, Nov. 1972, pp. 337–347.

[16]Mani, R., "The Influence of Jet Flow on the Jet Noise, Part II, the Noise of Heated Jets," *Journal of Fluid Mechanics*, Vol. 76, Feb. 1976, pp. 779–793.

[17]Gliebe, P. R., and Balsa, T. F., "The Aerodynamics and Acoustics of Coaxial Jet Noise," AIAA Paper 76-492, July 1976.

[18]Goldstein, M. E., "The Low Frequency Sound from Multipole Sources in Axisymmetric Shear Flows," *Journal of Fluid Mechanics*, Vol. 70, Aug. 1975, pp. 595–604.

[19]Balsa, T. F., "The Acoustic Field of Sources in Shear Flow with Application to Jet Noise: Convective Amplification," *Journal of Fluid Mechanics*, Vol. 79, Jan. 1977, pp. 33–47.

[20]Goldstein, M. E., "The Low Frequency Sound from Multipole Sources in Axisymmetric Shear Flows—Part II," *Journal of Fluid Mechanics*, Vol. 75, May 1976, pp. 17–28.

[21]Goldstein, M. E., *Aeroacoustics*, McGraw-Hill, New York, 1976.

[22]Tester, B. J., and Morfey, C. L., "Developments in Jet Noise Modeling—Theoretical Predictions and Comparisons with Measured Data," *Journal of Sound and Vibration*, Vol. 46, No. 1, 1976, pp. 79–103.

[23]Pao, S. P., "Aerodynamic Noise Emission from Turbulent Shear Layers," *Journal of Fluid Mechanics*, Vol. 59, July 1973, pp. 451–479.

[24]Goldstein, M. E., "High Frequency Sound Emission from Moving Point Multipole Sources Embedded in Arbitrary Transversely Sheared Mean Flows," *Journal of Sound and Vibration*, Vol. 80, No. 4, 1982, pp. 499–522.

[25]Balsa, T. F., "The Far Field of High Frequency Convected Singularities in Sheared Flows, with an Application to Jet Noise Prediction," *Journal of Fluid Mechanics*, Vol. 74, March 1976, pp. 193–208.